



Published in final edited form as:

Ann Biomed Eng. 2020 January ; 48(1): 225–235. doi:10.1007/s10439-019-02333-x.

Acoustic Emissions as a Non-Invasive Biomarker of the Structural Health of the Knee

Daniel C. Whittingslow^{1,2,*}, Hyeon-Ki Jeong³, Venu G. Ganti³, Nathan J. Kirkpatrick¹, Geza F. Kogler⁴, Omer T. Inan^{2,4}

¹Coulter Department of Biomedical Engineering, Georgia Institute of Technology and Emory University, Atlanta, Georgia

²Emory University School of Medicine

³School of Electrical and Computer Engineering, Georgia Institute of Technology, Atlanta, Georgia

⁴School of Biological Sciences, Georgia Institute of Technology, Atlanta, Georgia

Abstract

The longitudinal assessment of joint health is a long-standing issue in the management of musculoskeletal injuries. The acoustic emissions (AEs) produced by joint articulation could serve as a biomarker for joint health assessment, but their use has been limited by a lack of mechanistic understanding of their creation. In this paper, we investigate that mechanism using an injury model in human lower-limb cadavers, and relate AEs to joint kinematics. Using our custom joint sound recording system, we recorded the AEs from 9 cadaver legs in four stages: at baseline, after a sham surgery, after a meniscus tear, and post-meniscectomy. We compare the resulting AEs using their b-values. We then compare joint anatomy/kinematics to the AEs using the x-ray reconstruction of moving morphology (XROMM) technique. After the meniscus tear the number and amplitude of the AE peaks greatly increased from baseline and sham (b-value = 1.33 ± 0.15 ; $p < 0.05$). The XROMM analysis showed a close correlation between the minimal inter-joint distances (0.251 ± 0.082 cm during extension, 0.265 ± 0.003 during flexion, at 145°) and a large increase in the AEs. This work provides key insight into the nature of joint AEs, and details a novel technique and analysis for recording and interpreting these biosignals.

Keywords

Wearable sensing; Musculoskeletal assessment; Cadaver Model; XROMM; Diagnostic; Predictive; Prognostic Markers

Terms of use and reuse: academic research for non-commercial purposes, see here for full terms. <https://www.springer.com/aam-terms-v1>

*Correspondence should be addressed: dcwhitt@emory.edu.

Competing interests: The authors have no competing financial interests to report.

Data and materials availability: The authors will make the data available upon request.

Publisher's Disclaimer: This Author Accepted Manuscript is a PDF file of an unedited peer-reviewed manuscript that has been accepted for publication but has not been copyedited or corrected. The official version of record that is published in the journal is kept up to date and so may therefore differ from this version.

Introduction

The knee is one of the most frequently injured body parts, with 18 million knee related patient visits occurring per year in the United States (2). However, the number of acute knee injuries pales in comparison to the number of people suffering from chronic joint diseases such as osteo- and rheumatoid arthritis. It is predicted that by 2040 26% of the overall population will be diagnosed with some form of arthritis in the United States (16). This prevalence coupled with the severe reduction in quality of life presents a significant burden on patients and healthcare systems (30). Currently, clinical assessment and treatment relies on qualitative mobility assessments, patient reported symptoms, and imaging studies. A suitable marker of knee joint health that is quantitative, and measured with affordable hardware, could reduce this burden on healthcare systems and greatly improve patient outcomes and quality of life.

One such possible marker of knee joint health is the acoustic emission signature produced by knees during movement. These joint sounds have been explored as a means of assessing the joint's structural health since at least 1902 when Blodgett reported on auscultating the knee (4). Since then, researchers have employed a wide range of instruments and analysis techniques to detect and interpret the sounds produced during movement of the knee. These findings have often led to attempts to diagnose joint conditions (19,20). However, the ability to interpret acoustic emissions from the knee for clinical decisions has had limited success. One of the main reasons for this is a lack of mechanistic understanding of how these joint sounds are produced and what factors influence them.

In this paper we investigate joint acoustic emissions using a human lower-limb cadaver model to address this knowledge gap in the field. This model allows for highly controlled analysis of the joint sounds from the knee in a reproducible and anatomically relevant manner. To record the acoustic emissions, the limb is fixed to a platform and passively flexed/extended through its range of motion with contact microphones sutured medial and lateral to the patellar tendon. The sounds produced during this movement are recorded and are the focus of this paper.

To better understand the source of these joint sounds, we explore the relationship between internal contact of the articulating structures within the knee and acoustic emission. This is done using a system of inertial measurement units (IMUs), biplanar motion capture x-ray imaging, and computed tomography (CT) scans. The output from that system is synced with the acoustic emission data. To observe the changes in acoustic emissions from the knee, we created a medial meniscus injury model to better understand how alterations of the underlying anatomy can correlate with the acoustic emissions recorded on the surface of the knee. Combining literature on internal joint pressure, our findings of minimum articulating surface distances, and joint sounds at each stage of injury led to our proposed model of joint sound production (Fig 1). To provide more physiologic context to the model, we next emulated the biomechanical alterations associated with swelling following an acute injury by serially injecting saline into the joint capsule. The b-value of the acoustic emissions was calculated at each stage of testing. This metric represents the scaling of the amplitude

distribution of the signal and was previously shown to be able to differentiate between knee statuses (17).

This paper represents the first time that an analysis of knee acoustic emissions has been performed on a controlled, cadaver model with incorporation of anatomical complexity, confounding physiological factors that occur in an injured state (i.e. swelling), and specific structural changes in the knee. Our findings allowed us to propose a model of knee acoustic emission that better localized the source of these sounds while remaining consistent with the prior literature's findings that these sounds can be useful in classifying the health status of a knee (15,17). Future work will include measurements of acoustic emissions from various knee injuries to better understand diagnostic capabilities of this modality. If characteristic alterations of these acoustic emissions can be linked with knee health status, joint sounds may offer a surrogate biomarker for early detection and assessment of musculoskeletal injury.

Materials and Methods

Cadaver Specimen Procurement and Preparation

Experiments were conducted on 9 fresh, frozen human cadaver lower-limbs. The specimens were procured from MedCure, Inc (Orlando, FL, with permission for use in a research experiment), had an average age of 63.6 ± 9.5 years of age, stored at -20°C , and thawed to room temperature in a water bath for 8 h prior to testing. The age of these cadaver specimens may not be fully representative of the overall population, but the exclusion criteria helped limit the impact of confounding comorbidities. The joints were selected from donors with no known arthritis, injuries or past surgeries of the knee, and that were mobile at time of death. Prior to use, the legs were clamped to the laboratory benchtop and preconditioned with manual flexion/extension movements for five minutes.

Knee Acoustic Emission Setup and Acquisition

Two uniaxial analog accelerometers (3225F7, Dytran Instruments Inc. Chatsworth, CA) were sutured (4-0 Nylon Kit, Your Design Medical, Brooklyn, NY) 2 cm medial and lateral to the patellar tendon. These accelerometers have a broad bandwidth (2Hz-10kHz), high sensitivity (100 mV/g), low noise floor (700 μgrms), miniature size and low weight (1 gram). The medial and lateral patellar locations were selected due to the relatively unimpeded route (only a thin layer of muscle, tendon, and fat) to the articulating surface of the knee (where intra-joint friction is thought to produce the recorded vibrations (19)).

To record the knee acoustic emissions, the cadaver legs were suspended on the side of a lab bench and passively flexed and extended through their full range of motion ($\sim 90^{\circ}$ to 180°) (Fig 2). This suspension ensured the cadaver limb and especially the foot did not contact the surface of the lab bench at any stage of the motion. To pre-condition the leg prior to sound recording, it was flexed/extended through its full range of motion for 5 minutes at a rate of 1 cycle every 4 seconds. After pre-conditioning the acoustic emission recording began. The legs were extended for two seconds, and then flexed through the same range for two seconds; thus, one flexion/extension cycle occurred every 4 seconds. The recordings

contained a total of ten flexion/extension cycles with 5 seconds of background, environment noise recorded before and after the exercise for a total recording time of 50 s. An inertial measurement unit (MPU6050, TDK InvenSense, San Jose, CA) was attached 5 cm proximal to the ankle and used to validate the joint angle and rotational velocity during these exercises. The signals from the accelerometer were sampled at 100 kHz and recorded using a data acquisition module (USB-4432, National Instruments Corporation, Austin, TX)

Tear Protocol

Each of the knees (n=9) were serially, surgically altered in four stages to isolate the effects that a medial meniscus tear has on the joint's acoustic emissions. The four stages of testing were baseline, sham surgery, meniscus tear, and the meniscectomy. After thawing and pre-conditioning, the joint sounds were first recorded at their baseline status. Next, a sham surgery was performed on the leg. The sham surgery was performed with the knee at 90° of flexion with a 5-cm oblique incision made just posterior to the superficial medial collateral ligament (MCL) at the level of the vastus medialis curving over the medial epicondyle onto the anteromedial aspect of the tibia. This cut exposed the interval between the posteromedial joint capsule, semimembranosus, and medial head of the gastrocnemius (23). Next, the posteromedial joint capsule was cut 2 cm to expose the medial meniscus. Without damaging the meniscus, the incisions were closed with simple continuous, running sutures (25). The sounds were recorded at this sham surgery status. Next, the meniscus tear was introduced. The sutures were cut to re-expose the meniscus and a 10mm transverse (radial) incision on the posterior (zone A) portion of the meniscus was performed. The surgical entry path was again sealed with a simple continuous running suture and the sounds were recorded. Finally, a meniscectomy was performed on the injured meniscus. The sutures were cut to re-expose the meniscus and a 5mm margin anterior and posterior to the transverse/radial meniscus cut was surgically removed. The incisions were resealed and sounds re-recorded.

Saline Injection Protocol

To emulate the altered mechanical environment within the knee resulting from swelling following acute injury (8,12), varying levels of saline were injected into the knees prior to meniscus surgery (n=5). A superolateral approach into the suprapatellar pouch was used due to its reliability as a route of entry into the knee joint and the obstruction of the attached microphones impeding other approaches (27). The leg was fully extended and a 1.5 in 25-gauge needle was inserted underneath the superolateral surface of the patella and directed posteriorly and inferomedially into the knee joint. 5 mL aliquots of saline were serially injected from 0 to 50 mL. After each injection, the joint sounds were recorded using the above acoustic emission acquisition protocol.

Acoustic Data Pre-Processing

The recorded signals were analyzed using Matlab (MathWorks, Natick, MA). The signals were pre-processed using a digital finite impulse response (FIR) band-pass filter with 250Hz - 20kHz bandwidth to maintain emissions in the audible range while removing motion artifacts. This frequency range was previously shown to contain the relevant knee acoustic emissions information (28). Once filtered, the signals were synchronized to the IMU data and trimmed to remove the excess periods of noise before and after the flexion/extensions.

This trimmed noise was then used as a basis for a noise suppression algorithm using spectral subtraction from the acoustic emission recordings (5).

b-value Analysis of Acoustic Data

The b-value metric was computed for the acoustic emissions to differentiate the sounds based on their amplitude distribution of the acoustic emissions. The b-value was first proposed by Gutenberg and Richter in earthquake seismology to quantify a logarithmic relationship between the magnitude and frequency recorded in a seismic trace, using the empirical formula expressed in Equation 1 (13).

$$\log_{10}N = a-bML \quad \text{Equation 1.}$$

Where ML is the Richter magnitude of events, N is the number of events with magnitudes greater than ML, and a and b are the constants. Based on this relationship, the b-value is the negative gradient of the log-linear acoustic emissions frequency/magnitude plot and thus represents the slope of the amplitude distributions. Our previously published work successfully used the computed b-value of joint sounds to differentiate knee injury status in athletes (17).

Acoustic Data Statistical Methods

The mean and standard deviation were calculated for each dataset. The data were assessed for normality using a Lilliefors test. It was found that the groups were non-normal, so the Scheirer-Ray-Hare extension of the Kruskal Wallis test was performed. This test is often used as a non-parametric equivalent to the two-way analysis of variance (ANOVA) test. Finally, multiple Wilcoxon signed rank tests were performed to compare between the data groups. A Bonferroni correction was applied to correct for the multiple comparisons. The same series of tests were performed on the saline injection data.

Joint Distance Imaging

The geometry of the tibial plateau is complex and asymmetric. In order to calculate the distance between the femur and tibia during articulation we used a two-part imaging protocol relying on a high-speed, biplanar x-ray video (100 fps, 79° between beam angle) and a computed tomography (CT) scan of the patella, tibia, and femur. Three 1mm diameter, radiopaque, tantalum markers (X-Medics, Frederiksberg, Denmark) were implanted into each bone on the posterior-medial, posterior-lateral, and anterior aspects of the bone. These three markers appeared in both the CT scan and x-ray videos. The CT scan allowed for a 3D model of the bones to be constructed. These markers were tracked in the x-ray videos using XMA Lab (Brown University, Providence, RI) and aligned with the markers on the CT-derived 3D model using Maya (Autodesk, San Rafael, CA) in order to track the complex interaction between the bones. This motion tracking technique is known as X-ray Reconstruction of Moving Morphology (XROMM) (6,18). With the articulation of the bones fully visualized using XROMM, the distances between each of the 7076 vertices of the triangles making up the 3D mesh of the tibial plateau and its nearest femoral counterpart were calculated using custom Python scripts.

Results

In this study, the effects of a meniscus tear on the acoustic emissions produced by manually articulating a human cadaver knee are explored. The results from these tests are presented below. The b-value is the principle metric for comparison. It is a unitless metric that describes the slope of the amplitude distribution of an acoustic signal.

Sham surgery on a cadaver model of joint acoustic emissions does not significantly alter the acoustic emissions from a baseline state

A sham surgery was performed to expose the medial meniscus of the cadaver. All the successive layers from the skin to the joint capsule were surgically resected (Fig 3 A/E to Fig 3 B/F), and the acoustic emissions were recorded. Qualitatively, the time domain sound signature at this stage of testing appears very similar to the baseline state (Fig 3 J). The b-value statistic of the joint sounds at baseline was 1.99 ± 0.54 . After the sham surgery, the b-value dropped to 1.87 ± 0.40 . This shift was not statistically significant ($p=0.25$). This lack of statistical significance indicated that the sham surgery, with its alteration to the tissue external to the joint cavity and exposure of the joint capsule to the air and laboratory atmosphere, had minimal influence on the acoustic emissions of the knee.

Introducing a meniscus tear significantly alters the acoustic emissions from the sham state

A full width, radial tear was performed on the posterior, medial meniscus (Fig 3 B/F to Fig 3 C/G). After closing the resection, the sounds produced by the knee were again recorded and analyzed. At this stage, the sounds appear much more chaotic, with several large spikes in the amplitude of the sounds. This increase in amplitude was reflected in the b-value after the meniscus tear ($b\text{-value} = 1.33\pm 0.15$). This drop in the b-value was significant when compared to the baseline and sham stages ($p=0.0039$). This significance indicated that the meniscus tear was solely responsible for the change seen in the acoustic emissions. It indicates that knee acoustic emissions are capable of differentiating the internal environment of the knee.

Further removal of the meniscus via meniscectomy does not significantly alter the acoustic emissions

After the meniscus cut was completed, the cadaver was reopened and a larger portion (with clean margins) of the torn meniscus was removed resembling a meniscectomy (Fig 3 C/G to Fig 3 D/H). Qualitatively, the acoustic signal appeared to diminish at this stage from the meniscus tear state (Fig 3 L). When analyzed, there was a marginal increase in the b-value (1.34 ± 0.29) toward the baseline/sham values. However, this increase was statistically insignificant when compared to the meniscus tear group ($p=0.91$). This indicates that the size of the meniscal defect or border tear patterns may not significantly alter the acoustic emissions of the knee.

Saline injected within the knee capsule as a surrogate for effusions does not significantly impact acoustic emissions

After a meniscus tear occurs *in vivo*, a series of physiologic events begin in response to the injury. Principal among these regarding the effect on mechanical articulation is localized swelling. To better understand the extent to which this swelling affects joint acoustic emissions we serially injected 5 mL aliquots of 0.9% saline solution into the knee capsule. (Fig 4 A). After each injection, the acoustic emissions were recorded and b-value calculated. The b-values ranged from a minimum of 1.6 ± 0.3 to 2.1 ± 0.6 . The data were highly variable with no clear trends or statistical significance ($p > .05$ for $n=5$) (Fig 4 B). Therefore, the injection of saline into the knee capsule does not directly influence the production or propagation of acoustic emissions

The distance between the femoral condyles and tibial plateau is minimized when the knee is between 140° and 150°

The tibio-femoral distance was measured on one of the cadaver legs using the X-ray Reconstruction of Moving Morphology (XROMM) imaging analysis technique on one of the cadaver legs (6,18). Distances from the tibial plateau to the nearest point on the femur were computed for 7076 vertices that made up the tibial plateau of the CT-derived 3D model. We found that the distance between the two articulating structures was minimized between 140° and 150° during both flexion and extension. The point distances at three demonstrative angles during extension (120°, 150°, and 180°) are presented as a heat map (Fig 5 A). Of note, the minimum distances (darker red) trend to the anterior as the leg articulates. This agrees with reported tibiofemoral distances in the literature (1,10,21,24). For reference, the posteromedial meniscus tear was located on the bottom-left portion of the tibial plateau as presented in Fig 5A. Of note, the minimum dimensions did not significantly change between any stages of the experimental protocol (Fig 5 D,E). This indicates that the interventions did not cause significant changes in the biomechanics and articulation pattern of the cadaver leg.

The RMS power of the acoustic waveform and the rate of change of the minimum tibiofemoral distances differed during the extension and flexion phases of movement. The minimum tibiofemoral distance during extension is 0.251 ± 0.082 cm and during flexion is 0.265 ± 0.003 cm both occurring at 145° (Fig 5 B,C). The tibiofemoral distance sharply increased from the minimum at 145° to 180° (full extension) during both the flexion and extension phases of movement. During extension, there is a large increase in the RMS power from when 145° to full extension. This increase in RMS power mirrors the increase seen in the extension-phase tibiofemoral distance plot (Fig 5 B, D). The relationship between RMS power of the acoustic signal and distance is slightly different during the flexion phase of movement. During flexion, the peak in RMS power of 0.34 ± 0.02 occurs at 150° flexion nearly coinciding with the minimum tibiofemoral distance at 145° flexion. During flexion we again note an increase in the rate of growth of the RMS power from 160° to 150° - closely resembling the rate of change in the tibiofemoral distance plot. The difference in the relationship between RMS power and tibiofemoral distance during the flexion and extension phases along with the slight delay in the RMS power of the signal following maximum compression indicates that there is a more complex interaction occurring to create these joint acoustic emissions than rigid-body bone-on-bone compression alone.

Discussion

Meniscal tears are the most common knee injury, and partial meniscectomies are one of the most common orthopedic surgical procedures. These injuries are seen in all age groups and have a variety of causes (22). The primary functions of the menisci are load distribution and stability during ambulation. Upon injury, the menisci have an impaired ability to distribute loads and resist tibial translation – destabilizing the joint. During extension, the medial and lateral menisci transmit 50% and 70%, respectively, of their compartmental loads. During flexion those increase to 85% and 90% respectively (26). It has previously been shown that after medial meniscectomy, contact stresses can increase by 100% (4). Meniscal tears can be described as one of six morphologies: radial, oblique, horizontal, complex, vertical, or bucket handle. The type of tear has been shown to have a significant effect on contact pressures within the knee. In particular, complete radial tears significantly increase mean contact pressure and decrease contact area compared with the intact state (22). Significant research has been performed on tear morphologies (9,14), compartment pressures (3,11), and outcomes of different corrective surgical approaches (22).

Diagnosis of meniscal injury is made clinically based on the patient's history (e.g. description of pain/timing), a physical examination (e.g. gait analysis, lower extremity alignment, range of motion analysis), and imaging tests (e.g. magnetic resonance imaging (MRI) and radiographs) (26). This diagnostic workup is extensive, but not without its shortcomings. The patient's history and their pain ratings are highly subjective. The physical exam is dependent on the practitioner's expertise. The MRI is by far the most powerful and objective tool for evaluating the meniscus; however, it is time-consuming, costly, and often uncomfortable for the patient. Post-surgical monitoring and rehabilitation efforts rely on the same assessment techniques, typically with even fewer imaging studies. We believe that the acoustic emissions produced by the knee during flexion/extension could serve as a suitable marker of knee joint health that is quantitative, affordable, and easily incorporated into a clinical assessment.

The acoustic emissions explored in this paper were produced by the articulation of the tibiofemoral joint. This joint is a hinge synovial joint that joins the distal femur to the proximal tibia. The articulation occurs between the medial and lateral femoral condyles and the tibial condyles. The friction during this articulation creates a complex series of vibrations (37). These vibrations travel to the skin where they encounter a large impedance mismatch between the tissue and air and manifest as vibration signals on the skin (27). In this paper, we proposed a cadaver injury model to better understand the impact that factors such as injury and swelling have on these acoustic vibrations. In addition, the tibiofemoral distances during movement were measured and correlated to the acoustic emissions. This was the first time that human knee acoustic emissions have been studied in such a controlled setting.

To record these skin vibrations, our team designed a system that incorporates two uniaxial accelerometers acting as contact microphones to record these vibrations. To provide anatomical context to the recorded sounds an IMU simultaneously and synchronously

recorded the angle of the cadaver legs while they were manually flexed and extended through their ranges of motion.

Our exploration of knee acoustic emissions began with a four-stage surgical intervention. We had previously shown that injuries to the knee resulted in significant alterations to the acoustic emissions as measurable by the b-value metric (17). On 9 fresh-frozen cadaver legs, the sounds were first recorded at baseline after the legs were pre-conditioned and thawed in a water bath. A sham surgery was performed to expose but not damage the medial meniscus. The lack of significant changes between the acoustic signals from baseline to sham indicated that the exposure of the meniscus with the cutting of the various skin and fascial layers was not responsible for the bulk of the acoustic emissions. Next, we re-entered and performed a 10mm radial incision on the meniscus. With the meniscus torn, the acoustic emissions significantly increased, and this meniscus-torn state was easily differentiated using the b-value metric. In the final stage, we removed a 5 mm margin around the meniscus tear. This removal resembles a surgical meniscectomy – the commonly performed reparative surgery for this type of injury. After meniscectomy, the b-value of the acoustic emissions returned toward baseline but was still not significantly different from the meniscus cut stage. This lack of significant change in the b-value following meniscectomy indicates two possible outcomes: 1) The cadaver model was not a suitable substitute for a reparative treatment given the lack of blood flow/synovial fluid, or 2) this sensing modality may not be suitable for monitoring post-surgical repairs. In earlier work, the knee acoustic emissions were recorded from athletes at the start of their season and after suffering injuries such as torn anterior cruciate ligaments, torn menisci, and sprained medial collateral ligaments. In that study we found that the b-value and this sensing modality was able to track their recovery post-surgical intervention (15,17). Thus, the lack of return toward baseline is most likely due to differences in the physiology/anatomy of the cadaver model and young, collegiate athletes.

In an effort to examine this discrepancy in findings between athletes and cadaver model, we explored a possible confounding factor – swelling. Intra-articular knee joint effusions accompany nearly all knee injuries (29). The serial injections of 5 mL aliquots of 0.9% saline solution did not significantly alter the knee acoustic emissions. This was counter to our expectations. We had expected an increase in intra-joint fluid volume to lead to an increase in the tibiofemoral distance and less interactions between the articulating components in the knee thereby decreasing acoustic emissions. This lack of significance was promising for the sensing technology to be used clinically since the level of swelling will not need to be controlled for when interpreting joint acoustic emissions; however, it did present data counter to our prevailing notion of how these sounds were produced. This finding led to our interest in exploring the relationship between tibiofemoral distance and acoustic emissions.

To explore the relationship between anatomical distances and joint acoustic emissions a series of biplanar, video x-rays and CT scans were performed on a cadaver specimen. Following the XROMM protocol, tibial and femoral movements were tracked and segmented 3D models were animated using the x-ray videos as reference. The distance between the tibia and femur were calculated continuously through the leg's range of

movement (6,18). The RMS power of the joint acoustic emissions was calculated along each leg's range of movement for comparison. The RMS power metric of acoustic emissions was calculated rather than the b-value since the b-value relies on a longer signal with many peaks occurring. In Figure 5, the RMS power of the signal was calculated for every 2.5° of movement which amounted to a signal time of 55.4 ± 0.2 ms. Often, there were no large amplitude spikes in that small time interval and the b-value would tend toward infinity by virtue of its derivation. There was a slight delay in the increase in the RMS power after the minimum joint distance was reached. We believe that this delay in sound production may indicate that the sounds are a result of the viscoelastic expansion of the menisci. The mechanical properties of the meniscus have been extensively characterized (29). Principle among these analyses are the characterization of the complex viscoelasticity and anisotropy of the meniscus. We propose that knee acoustic emissions are heavily influenced by the compression of the menisci and the consequent release of compression during movement. The viscoelasticity of the meniscus may be responsible for the slight delay between the acoustic emission RMS spiking and the minimum tibiofemoral distance occurring.

In the future, the possibility of the viscoelastic properties of the meniscus contributing to the acoustic emissions of the knee will be further explored. If this theory is correct, its result may be far reaching in regard to diagnosing meniscal health from joint sounds. There may also be merit in correlating the acoustic emissions not only with experimentally measured tibiofemoral distances but also simultaneous, joint pressure mappings. In this work, we relied on previously published research to classify the pressure profile within the knee. Using experimental pressure data with our setup may provide a better correlation between the anatomical orientations and sounds produced. In order for this novel sensing modality to become clinically valuable, we need to discover the full extent of its capabilities both for longitudinal monitoring as well as diagnostics. The next steps in that development will involve expanding the scope of joint acoustic emission studies to different injuries and pathophysiological conditions (e.g., anterior cruciate ligament tears, arthritis, etc.). Future work should also focus on developing more sophisticated signal processing techniques for reducing noise, optimizing signal quality, and potentially isolating the sources of these sounds within the knee, so that the nature of these sounds can be better understood. Aside from clinical merit, there is also substantial intellectual merit to be gained by further researching the influence of confounding variables such as the ideal protocol for generating acoustic emissions, physiological variables such as pain, effusions, and degree of tear, and the ability to localize injuries based on an array of microphones. In the future, we intend to explore more fundamental acoustic emission analysis techniques to accurately and effectively characterize the differences between these responses.

The work in this paper presents the first time that knee acoustic emissions have been characterized in a controlled setting with a cadaver model of knee injury. The insights gained on the application of acoustic emissions for identifying meniscus tears are promising and warrant future work in the field. Additionally, the correlation of tibiofemoral distance to acoustic emission patterns provided the first of its kind attempt to correlate acoustic emissions with anatomical positions. The relation between joint anatomy, the associated interactions upon articulation, and the resulting acoustic emissions should be further explored to help understand the full utility of this novel sensing modality. With more

research, joint acoustic emissions could soon serve as a readily measurable, non-invasive biomarker of joint health.

Acknowledgements

The authors thank Professor Young-Hui Chang and his Comparative Neuromechanics Lab at the Georgia Institute of Technology for lending expertise on the imaging and XROMM tracking portion of this project. Funding: This work was supported by the National Institutes of Health, National Institute of Biomedical Imaging and Bioengineering, Grant No. 1R01EB023808, as part of the NSF/NIH Smart and Connected Health Program. Author contributions: DW served as the project lead and was involved in every part of its design, execution, and reporting. HJ was the lead data analyzer and assisted DW with the recording of the joint sounds. VG was involved in all aspects of the project, particularly the monitoring and execution of the articulations for proper sound recording. NK was the lead on the XROMM and imaging analysis portion of the project. GK conceived the original experimental cadaveric design model and provided clinical perspective on injuries to the knee. OI served as the principal investigator for the project, and was integral in the funding, managing, planning and execution of all aspects.

References

1. Ahmed AM, Burke DL. In-vitro measurement of static pressure distribution in synovial joints. *Journal of Biomechanical Engineering*. 1983; 105(3): 216–225. [PubMed: 6688842]
2. American Academy of Orthopaedic Surgeons. Information About Musculoskeletal Conditions. 3 11 2015.
3. Bai B, Shun H, Yin ZX, Liao ZW, Chen N. Changes of Contact Pressure in Patellofemoral Joint After Meniscectomies. *International Orthopaedics Journal*. 2012; 36: 987–991.
4. Blodgett W Auscultation of the knee joint. *Boston Medical Surgery Journal*. 1902; 146(3): 63–66.
5. Boll S Suppression of acoustic noise in speech using spectral subtraction. *IEEE Transactions on Acoustics, Speech, and Signal Processing*. 1979; 27(2): 113–120.
6. Brainerd EL, Baier DB, Gatesy SM, Hedrick TL, Metzger KA, Gilbert SL, and Crisco JJ. X-ray reconstruction of moving morphology (XROMM): precision, accuracy and applications in comparative biomechanics research. *Journal of Experimental Zoology*. 2010; 313(5): 262–279. [PubMed: 20095029]
7. Coluccino L, Peres C, Gottardi R, Bianchini P, Diaspro A, and Ceseracciu L. Anisotropy in the viscoelastic response of knee meniscus cartilage. *Journal of Applied Biomaterials*. 2017; 15(1): 77–83.
8. Dehaven KE, Diagnosis of acute knee injuries with hemarthrosis. *The American Journal of Sports Medicine*. 1980; 8(1): 9–14. [PubMed: 6892543]
9. Englund M, Roos EM, and Lohmander LS. Impact of type of meniscal tear on radiographic and symptomatic knee osteoarthritis. *Arthritis & Rheumatism: Official Journal of the American College of Rheumatology*. 2003; 48(8): 2178–2187.
10. Fairbank TJ Knee joint changes after meniscectomy. *The Journal of bone and joint surgery*. 1948; 30(4): 664–670.
11. Fukubayashi T, and Kurosawa H. The contact area and pressure distribution pattern of the knee. *Acta Orthopaedica Scandinavica*. 1980; 51(1–6): 871–879. [PubMed: 6894212]
12. Guilak F, Fermor B, Keefe FJ, Kraus VB, Olson SA, Pisetsky DS, and Weinberg JB. The role of biomechanics and inflammation in cartilage injury and repair. *Clinical Orthopaedics and Related Research*. 2004; 423: 17–26.
13. Gutenberg B, Richter CF. *Seismicity of the Earth and Associated Phenomena*. New York: Hafner Publishing Company 1965; 310.
14. Henry S, Mascarenhas R, Kowalchuk D, Forsythe B, Irrgang JJ, and Harner CD. Medial meniscus tear morphology and chondral degeneration of the knee: is there a relationship?. *Arthroscopy: The Journal of Arthroscopic & Related Surgery*. 2012; 28(8): 1124–1134. [PubMed: 22440795]
15. Hersek S, Pouyan MB, Teague CN, Sawka MN, Millard-Stafford ML, Kogler GF, and Inan OT. Acoustic emission analysis by unsupervised graph mining: a novel biomarker of knee health status. *IEEE Transactions on Biomedical Engineering*. 2018; 65(6): 1291–1300. [PubMed: 28858782]

16. Hootman JM, Helmick CG, Barbour KE, Theis KA, Boring MA. Updated projected prevalence of self-reported doctor-diagnosed arthritis, 2015–2040. *Arthritis Rheumatology*. 2016; 68: 1582–1587. [PubMed: 27015600]
17. Jeong HK, Whittingslow D, and Inan OT. b-Value: A Potential Biomarker for Assessing Knee Joint Health using Acoustic Emission Sensing. *IEEE Sensors Letters*. 2018.
18. Knörlein BJ, Baier DB, Gatesy SM, Laurence-Chasen JD, and Brainerd EL. Validation of XMA Lab software for marker-based XROMM. *Journal of Experimental Biology*. 2016; 219(23): 3701–3711. [PubMed: 27655556]
19. Krishnan S. Adaptive time-frequency analysis of knee joint vibroarthrographic signals for noninvasive screening of articular cartilage pathology. *IEEE Transactions Biomedical Engineering*. 2000; 47(6): 773–783.
20. Lee TF. Analysis of vibroarthrographic signals for knee osteoarthritis diagnosis; Proceeding 2012 6th International Conference Genetic Evolution Computing; 2012. 223–228.
21. Matsas A, Taylor N, and McBurney H. Knee joint kinematics from familiarised treadmill walking can be generalised to overground walking in young unimpaired subjects. *Gait & posture*. 2000; 11(1): 46–53. [PubMed: 10664485]
22. McDermott ID, Amis AA. The consequences of meniscectomy. *Journal of Bone and Joint Surgery*. 2006; 88:1549–1556.
23. Medvecky MJ, Noyes FR. Surgical approaches to the posteromedial and posterolateral aspects of the knee. *Journal of the American Academy of Orthopaedic Surgeons*. 2005; 13(2), 121–128. [PubMed: 15850369]
24. Perie D, Hobatho MC. In vivo determination of contact areas and pressure of the femorotibial joint using non-linear finite element analysis. *Clinical Biomechanics*. 1998; 13(6): 394–402. [PubMed: 11415814]
25. Post WR, Akers SR, and Kish V. Load to failure of common meniscal repair techniques: effects of suture technique and suture material. *Arthroscopy: The Journal of Arthroscopic & Related Surgery*. 1997; 13(6): 731–736. [PubMed: 9442327]
26. Rao AJ, Erickson BJ, Cvetanovich GL, Yanke AB, Bach BR Jr, and Cole BJ. The meniscus-deficient knee: biomechanics, evaluation, and treatment options. *Orthopaedic journal of sports medicine*. 2015; 3(10): 2325967115611386. [PubMed: 26779547]
27. Schumacher HR Jr. Aspiration and Injection Therapies for joints. *Arthritis Rheumatology*. 2003; 49(3): 413–20.
28. Teague CN, Hersek S, Toeryin H, Millard-Stafford M, Jones M, Kogler G, Sawka M, Inan O. Novel methods for sensing acoustic emissions from the knee for wearable joint health assessment. *IEEE Transactions on Biomedical Engineering*. 2016; 63(8): 1581–1590.
29. Torry MR, Decker MJ, Viola RW, O'Connor D, and Steadman JR. Intra-articular knee joint effusion induces quadriceps avoidance gait patterns. *Clinical Biomechanics*. 2000; 15(3): 147–159. [PubMed: 10656976]
30. Woolf AD, Akesson K. Understanding the burden of musculoskeletal conditions. *BMJ*. 2001; 322: 1079–1080. [PubMed: 11337425]

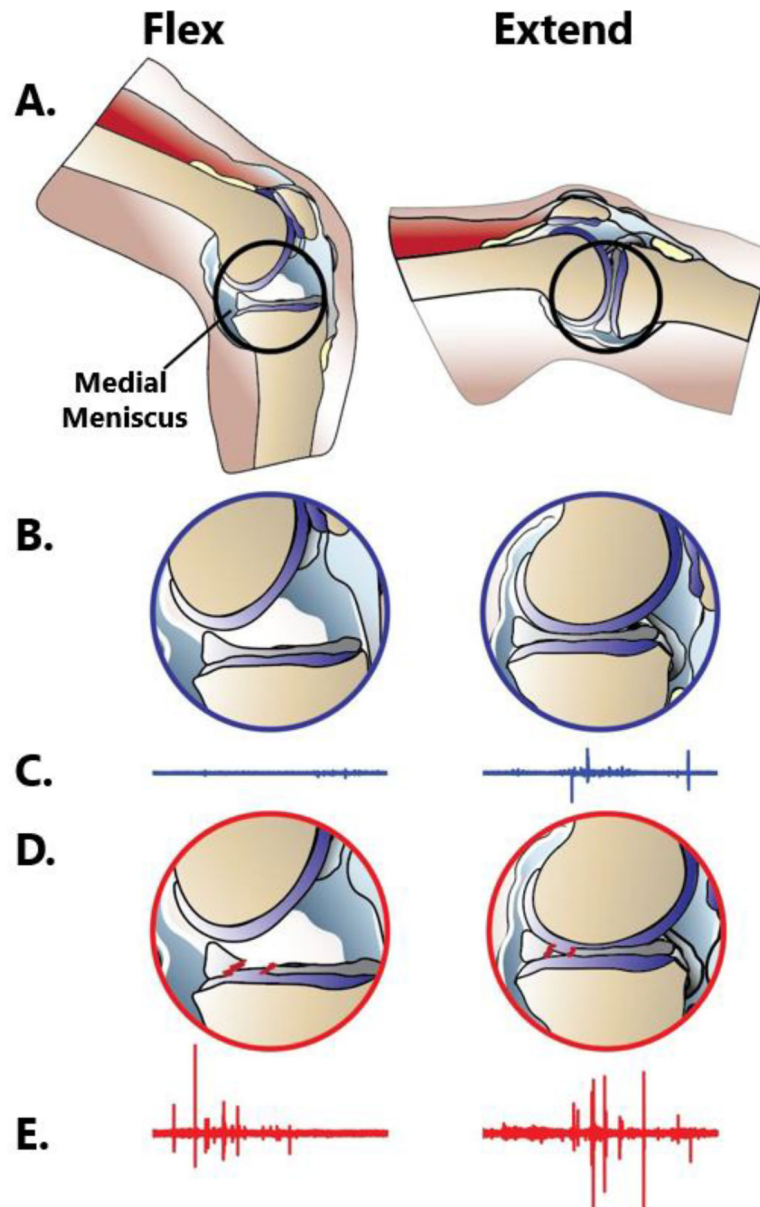


Fig. 1. Concept model of knee acoustic wave creation before and after a meniscus tear with representative acoustic wave forms.

A. Diagram of the knee during flexion and extension. **B.** Medial femoral condyle compressing the medial meniscus from flexion to extension. **C.** Representative acoustic waveform produced by the knee's movement. **D.** Compression of the radially-torn, medial meniscus from flexion to extension. **E.** Representative acoustic waveform produced by the knee.

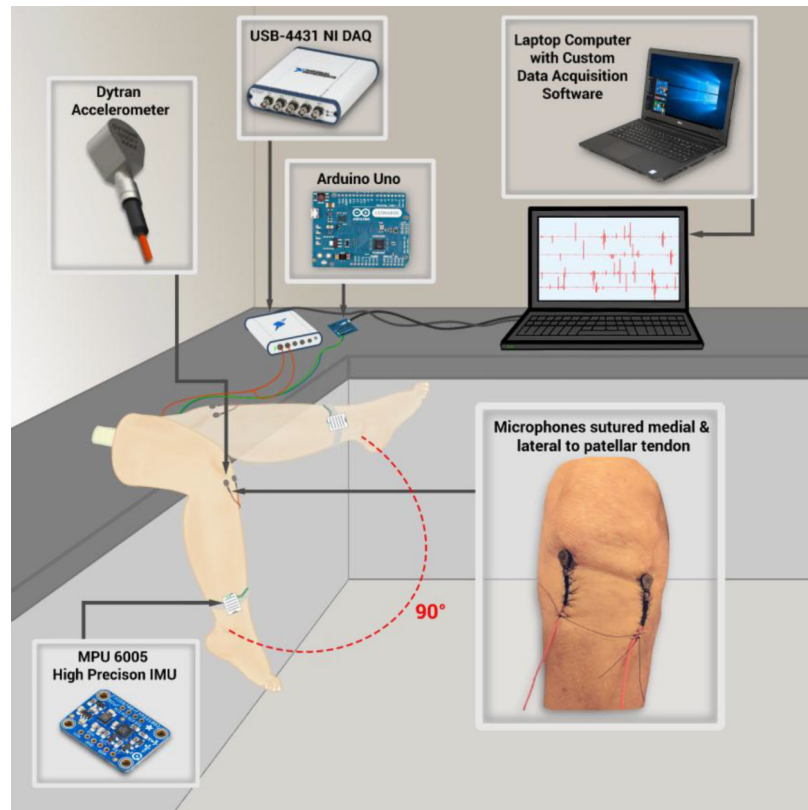


Fig. 2. Testing setup for the generation, acquisition, and analysis of knee acoustic emissions on a cadaver model.

The cadaver knee is outfitted with two accelerometers and a high-precision inertial measurement unit (IMU). The accelerometers are sutured medial and lateral to the patellar tendon and record the surface vibrations (acoustic emissions) created by the manual flexion/extension of the leg. The IMU captures and syncs the 3D motion data to the joint sounds providing anatomical relevance to the recorded signals. A data acquisition unit captures the audio waveform data and a microcontroller captures the IMU data. All data is transmitted to a laptop computer with custom acquisition and analysis software written in MATLAB.

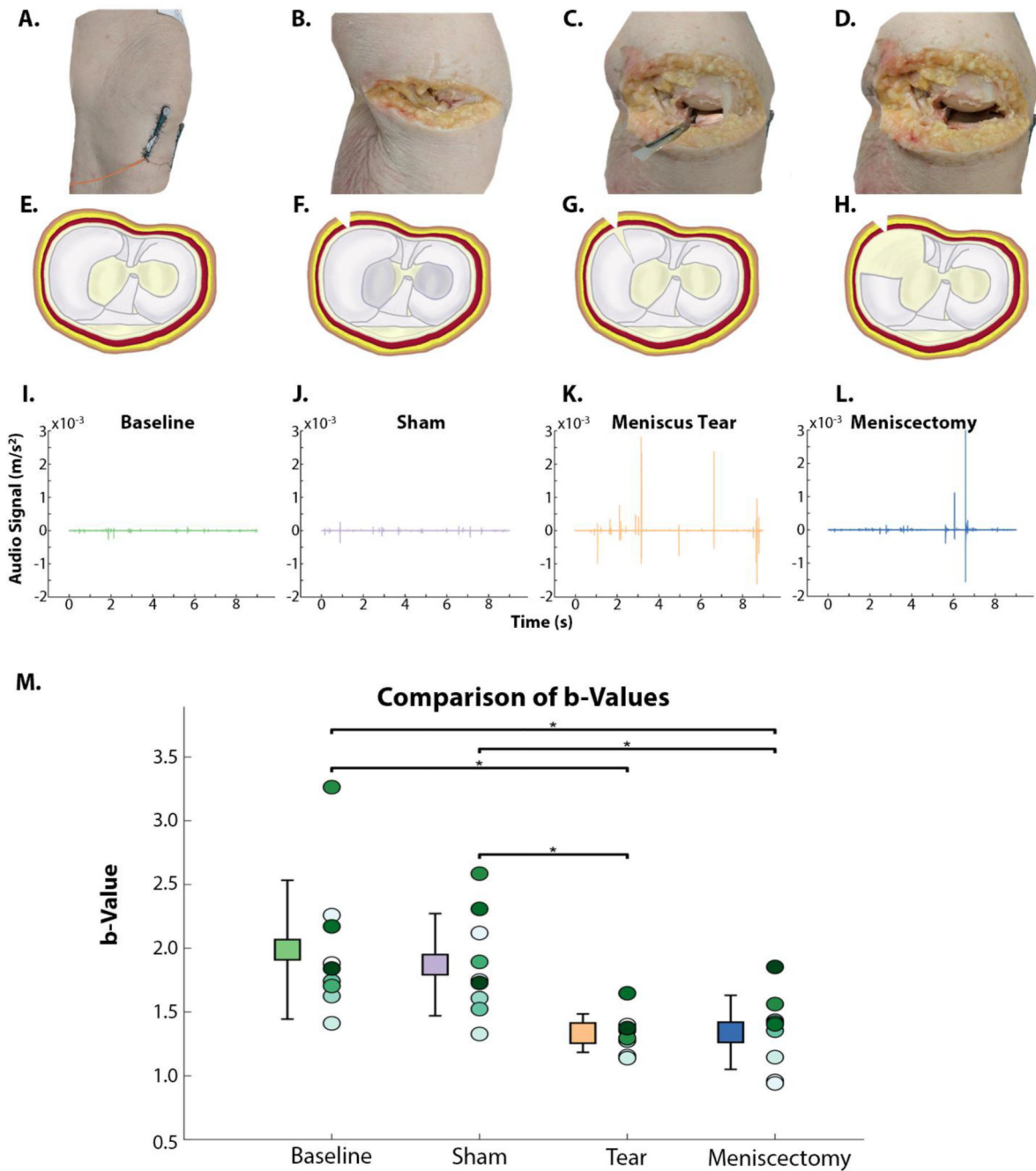


Fig. 3. Acoustic data and b-values from four stages of meniscus intervention: baseline, sham, meniscus tear, and meniscectomy. Surgical stages are presented as photos (A-D) and transverse plane view of tibial plateau diagrams (E-H). Each leg's AEs were recorded at baseline (A,E), after a sham surgery (B,F), after a posteromedial radial cut (C,G), and post-meniscectomy (D,H). Representative time-domain sound data from one flexion/extension cycle at each stage are presented in I-L. Note the increase in spikes and amplitude from baseline to meniscus tear (I-J) and slight decrease from tear to meniscectomy (K-L). There were statistically significant declines in the b-value from baseline to tear and meniscectomy, and from sham to tear and

meniscectomy. (indicated with *, n=9 and $p<0.05$). (error bars= 1 standard deviation from mean of the b-value from the 9 legs tested.)

Author Manuscript

Author Manuscript

Author Manuscript

Author Manuscript

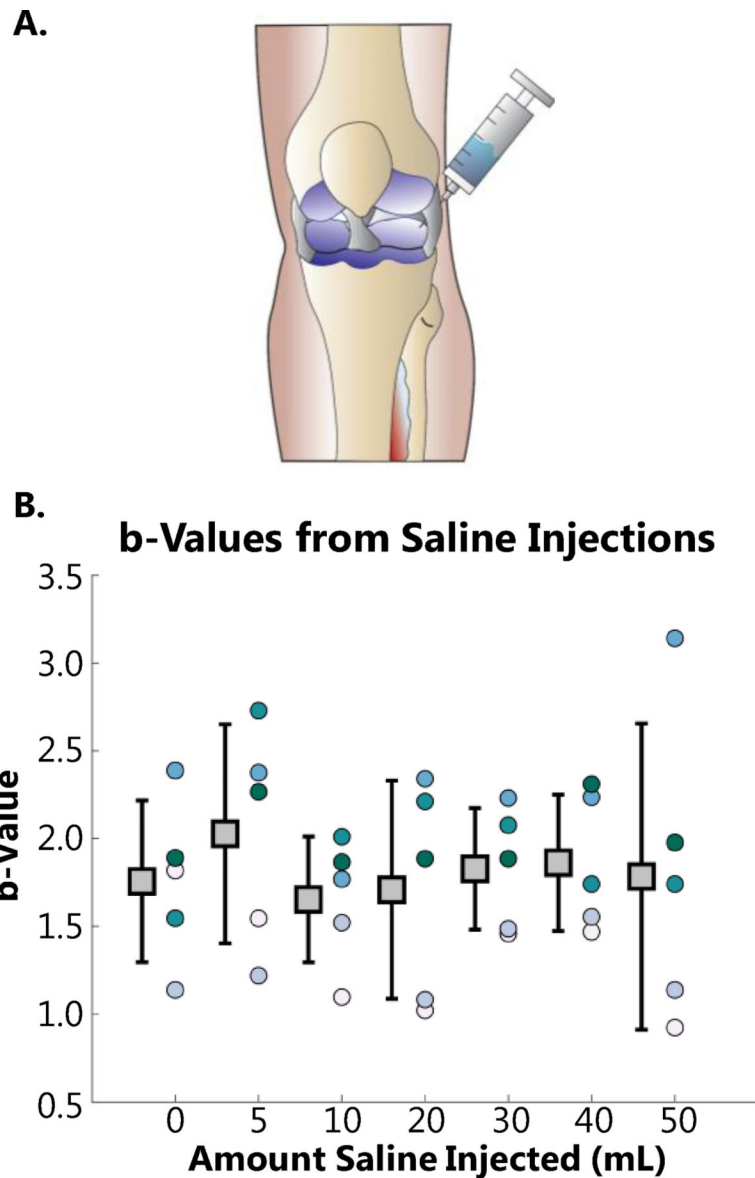


Fig 4. Acoustic Data and b-values from serial saline injections.

To emulate the mechanical effects of swelling on the acoustic emissions produced by the knee saline was serially injected from 0 to 50 mL into the joint cavity. The diagram in **A** demonstrates the superolateral approach used for injection of the saline. The corresponding b-values at each amount of injection are presented in **B**. There were no significant differences from 0–50 mL of injected saline indicating that there was not a statistically significant change in the acoustic emissions of the knee from this intervention. (n=5, error bars= 1 standard deviation from mean of the b-value from the 5 legs tested.)

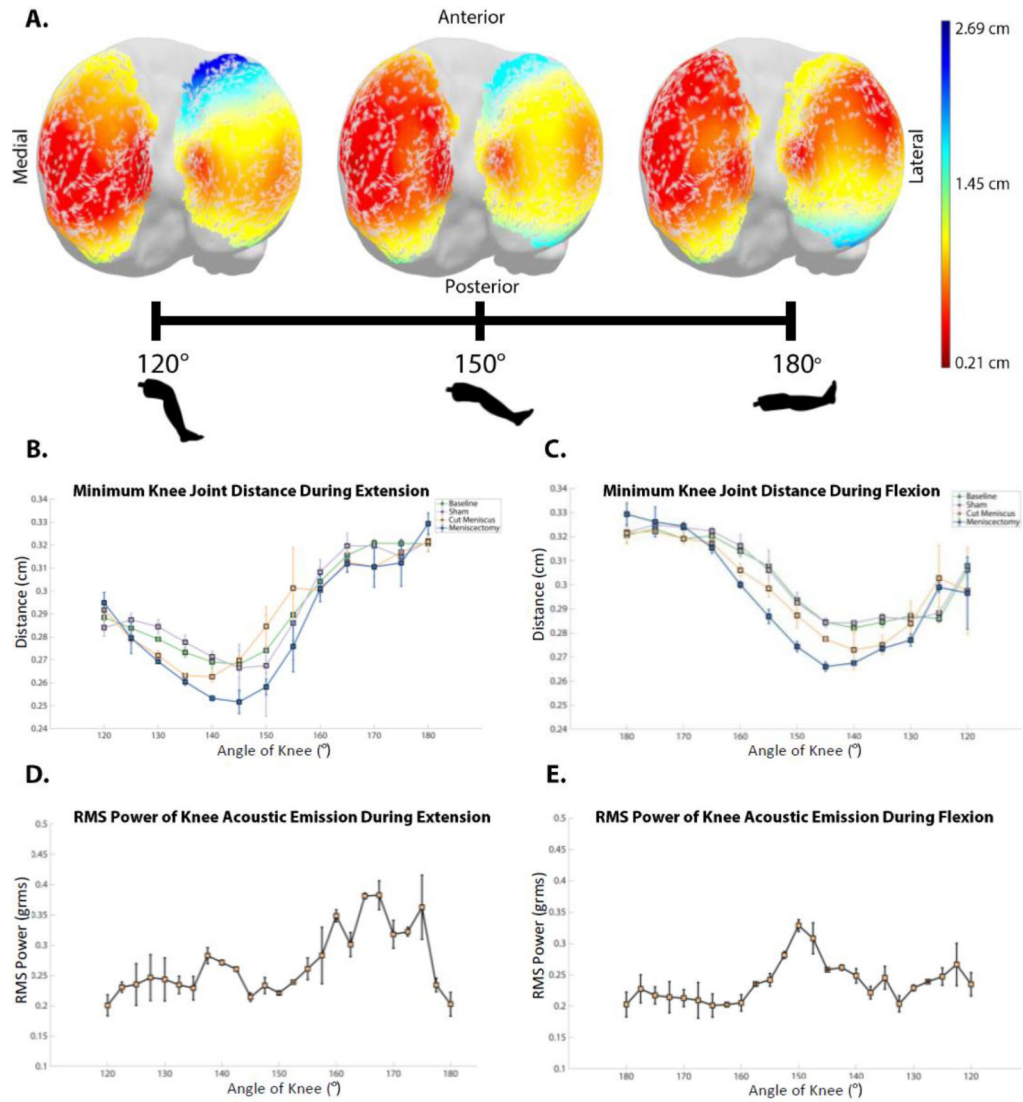


Fig 5. Comparison of tibiofemoral distances to sound recordings during a flexion-extension cycle. (A) Heatmap of distances from femoral condyles to tibial plateau at select distances (i.e. 120°, 150°, 180°). These heatmaps appeared nearly identical during flexion and extension. Minimum tibiofemoral distances at each degree of movement during (B) extension and (C) flexion (Error bars indicate one standard deviation from the mean of three trials at each data point). In B and C, the 1000 nearest vertices of the 7076 total vertices creating the 3D mesh are averaged with their standard deviations displayed. RMS Power of the joint acoustic emissions at each degree of movement during (D) extension and (E) flexion (Error bars indicate one standard deviation from the mean of the AEs of all n=9 cadaver legs tested.).